PHYSICAL REVIEW B

CONDENSED MATTER

THIRD SERIES, VOLUME 30, NUMBER 7 1 OCTOBER 1984

Electron-spin-resonance study of boron-doped amorphous Si_xGe_{1-x}:H alloys

M. Stutzmann and R. J. Nemanich

Palo Alto Research Center, Xerox Corporation, 3333 Coyote Hill Road, Palo Alto, California 94304

J. Stuke

Philipps-Universität, Renthof 5, D-3550 Marburg an der Lahn 1, Federal Republic of Germany

(Received 11 May 1984)

We report on ESR and Raman spectroscopy in a-Si_xGe_{1-x}:H prepared by glow discharge with a 1-vol% boron-doping level. For most silicon contents x, a preferential deposition of germanium into the solid film is found. The Raman spectra show that the samples are amorphous and that no phase separation is present. Four different ESR resonances can be observed over the compositional range investigated ($0<x<0.7$) at 20 K: the known resonances of the Ge dangling bonds and of localized holes in Ge—Ge bonding states, a signal due to carbon impurities, and a new resonance with strong negative g-value shift ($g=1.925$) that seems to be related to surface states. A model for the density of states in the amorphous Si-Ge alloys is proposed that can qualitatively account for the experimental results.

I. INTRODUCTION

Ever since amorphous silicon (a-Si) has been considered for commercial applications, amorphous silicon-germanium and silicon-carbon alloys (a-Si_xGe_{1-x} and a-Si_xC_{1-x}) have been of increasing interest also. This is because many of the electronic and optical properties of these materials can, in principle, be tuned to match external requirements by changing the alloy composition x. However, a common side effect of the alloying process between group-IV elements is an undesirable increase of the defect density in the band gap. Consequently, the majority of investigations has been directed towards an understanding of the optoelectronic properties and the nature of the defects of a given alloy.

In the case of a-Si_xGe_{1-x} alloys, experimental results exist for optical absorption, dark- and photoconductivity, photoluminescence, and photoinduced absorption,[1–9] as well as for more structure-related properties such as IR (infrared) absorption, hydrogen evolution, Raman scattering, annealing behavior, crystallization, and x-ray photoelectron spectroscopy (XPS).[10–16] As far as the nature of defects in the alloys is concerned, most of the current results have been deduced from electron-spin-resonance (ESR) measurements.[17–23] The ESR spectra allow at the same time an identification of the defects according to their g value and an evaluation of the defect density through the intensity of the ESR signal. ESR spectra of pure a-Si:H and a-Ge:H reveal the existence of three different characteristic paramagnetic states, depending on the position of the Fermi level.[24–27] In undoped samples the dangling-bond defect is predominant, whereas in phosphorus- or boron-doped material localized states of the conduction- or valence-band tail show up in the ESR spectra. As for the a-Si_xGe_{1-x} alloys, previous ESR studies have concentrated on undoped samples. The signatures of the observed defects can be understood in terms of an average property of the Si and Ge dangling bonds according to the composition x. Therefore, the g value and the peak-to-peak linewidth ΔH_{pp} of the alloy resonance change continuously from their values $g=2.0055$ and $\Delta H_{pp}=7$ G in a-Si to $g=2.022$ and $\Delta H_{pp}=40$ G in a-Ge. In investigating by ESR defects of the alloy system other than the dangling bond, the necessary shift of the Fermi level is again most easily obtained by gas-phase doping. To the best of our knowledge no systematic study of the ESR properties of doped a-Si_xGe_{1-x} exists so far. In this paper we have therefore investigated the changes in ESR spectra with alloy composition for a fixed doping level. Because the states of the valence-band tail appear to be much more localized than those of the conduction-band tail,[27] boron rather than phosphorus doping was used. Thus the observed spectra may be interpreted more in terms of the immediate surrounding of a given defect as opposed to the average properties of a larger region in the amorphous network. The experimental results reported here will allow us to address the question of the bonding structure in the amorphous alloy system. Moreover, a

model for the electronic density of states of a-Si_xGe_{1-x}:H will be discussed.

II. EXPERIMENT

Samples were prepared by rf glow discharge of a SiH_4-GeH_4-Ar gas mixture with volume ratios $x(g):1-x(g):1$. For doping the SiH_4-GeH_4 gas was premixed with 1 vol% B_2H_6. The deposition system (University of Marburg) was capacitively coupled. The following deposition parameters were used: rf frequency, 1.8 MHz; rf power, 4 W; pressure, 0.8 mbar; flowrate, 150 $cm^3 s^{-1}$; substrate temperature, 250°C.

Structure and composition of the obtained samples were investigated by electron-probe microanalysis (EPMA), scanning electron microscopy, and Raman spectroscopy. The ESR measurements were performed between 20 and 300 K with a Varian Associates model E-201 spectrometer (X band) in conjunction with an Oxford Instruments cryostat.

The ESR samples were prepared by peeling the deposited films off the molybdenum substrates and collecting the obtained flakes in narrow quartz tubes. For the Raman scattering experiments some of the flakes were pressed into small pellets because samples on suitable substrates were not available. The rough surface of these pellets caused a strong background in the Raman spectra due to elastically scattered light. Details of the Raman spectrometer are described elsewhere.[28]

III. RESULTS

Electron microscopy (resolution of 50 nm) showed the samples to be free of observable microstructure over the entire compositional range investigated. The results of Raman scattering and EPMA are summarized in Fig. 1. The upper part of this figure shows a typical Raman spectrum with three distinct peaks at the wave numbers 270, 380, and 460 cm^{-1}. The same structure has been observed by other investigators[8,10] and can be attributed to vibrational modes of Ge—Ge, Ge—Si, and Si—Si bonds, respectively. Using the Raman spectra of pure a-Si:H and a-Ge:H as reference points, an analysis of the three different Raman peaks in the alloy allows the determination of the relative numbers of related bonds and thus contains information about the composition $x(s)$ of the solid film. More precisely, for a continuous-random-network model[29] the number of the different bonds in a-$Si_{x(s)}Ge_{1-x(s)}$ is given by

$$\text{Ge—Ge: } 2N[1-x(s)]^2 , \tag{1a}$$

$$\text{Ge—Si: } 4Nx(s)[1-x(s)] , \tag{1b}$$

$$\text{Si—Si: } 2N[x(s)]^2 . \tag{1c}$$

Here, N is the total number of atoms. In Eqs. (1a)—(1c) the influence of the hydrogen bonded in the amorphous network has been neglected. The hydrogen concentration as determined by NMR amounts to typically 10—15 at.%. Since the Si and Ge atoms are fourfold coordinated, the total number of Si—Si, Si—Ge, and Ge—Ge bonds in a *hydrogenated* random network will be approximately 5% lower than predicted by (1a)—1(c). This deviation is negligible compared to the experimental uncertainty. Therefore we used the equations above without correction to determine the composition of the alloys from the Raman spectra.

In Fig. 1(b) the composition $x(s)$ thus derived is compared to the results of EPMA and plotted as a function of $x(g)$, i.e., the composition of the glow-discharge gas. Within the experimental errors [$\Delta x(s)=0.03$ for EPMA, $\Delta x(s)=0.1$ for Raman spectra] the two methods agree quite well. Moreover, the results of the Raman measurements can be used to exclude both phase separation and a significant microcrystallinity for the present alloys: Phase separation would lead to a suppression of the Ge-Si peak in the spectrum, and the presence of crystalline regions could be detected by a change in the shape and position of the observed peaks.

The deviation of the curve in Fig. 1(b) from the dashed line for $x > 0.06$ leads to the conclusion that in this region the deposition of a Ge atom is much more probable than that of a Si atom. A similar behavior has recently been observed for undoped a-Si_xGe_{1-x}:H prepared by glow discharge as well,[30] and it therefore seems to be an intrinsic property of this method of sample preparation not re-

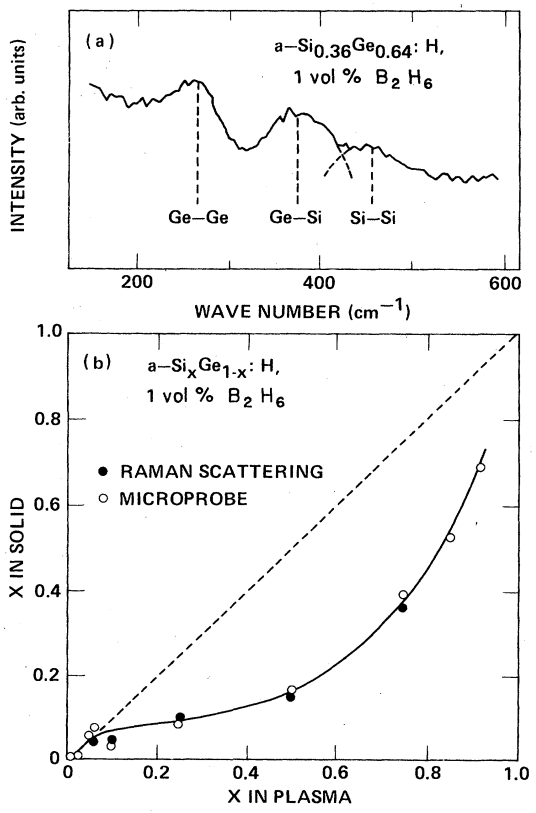

FIG. 1. (a) Raman spectrum of a-$Si_{0.36}Ge_{0.64}$:H showing the three peaks due to Ge—Ge, Ge—Si, and Si—Si bonds. (b) Silicon content $x(s)$ in the solid [determined by Raman scattering (solid circles) and electron-probe microanalysis (open circles)] as a function of the silane content in the gas phase.

lated to the presence of other gases (e.g., Ar and B_2H_6).

Turning now to the results of the ESR measurements, Fig. 2 shows a typical spectrum obtained from the alloy at low temperature (20 K). The relatively complex line shape can be analyzed in terms of four different resonances:[26] the resonance at $g=2.056$ ascribed to localized holes in the germanium valence-band tail, the Ge dangling-bond signal at $g=2.022$, a narrow signal at $g=2.003$ characteristic of carbon impurities, and a second broad resonance with a negative g-value shift ($g=1.925$). The existence of the latter signal, labeled X_1, is reported here for the first time. Although its microscopic origin remains unexplained so far, this resonance seems to be related to electronic surface states. The experimental evidence for this conjecture comes at this point from the fact that the resonance can be observed for a wide doping range in pure a-Ge:H (a similar resonance at $g=1.933$ can also be found in a-Si:H), and its intensity can be changed strongly by surface adsorbants.[31] As an example, Fig. 3 shows the change in the ESR spectrum of a sample with $x(s)=0.03$ (A) after 10 min contact with weak HCl (B). The amplitude of the X_1 resonance has been diminished by approximately 50%, and the g value has been shifted from 1.925 to the higher value of $g=1.933$ characteristic of a-Si:H. (Incidentally, the signal with $g=2.0026$ attributed to carbon impurities is affected by the surface treatment as well. This suggests that the underlying paramagnetic states are surface related also.)

The dependence of the spin density N_s on alloy composition is shown in Fig. 4 for the four resonances appearing in Fig. 2. At room temperature [Fig. 4(a)] only the Ge dangling-bond signal and the randomly changing resonance of the carbon impurities can be observed over the entire compositional range. The X_1 resonance appears only for Si contents smaller than 10 at. %, whereas the signal of the localized holes in Ge—Ge bonding states can only be detected for $x(s)>0.50$. Even though the silicon content in the deposited film approaches 70 at. %, none of the known a-Si resonances could be observed. The dependence of the amplitude of the different ESR signals on alloy composition becomes much clearer at low temperatures. The measured spin densities at $T=20$ K are shown in Fig. 4(b). At this temperature all four signals can be detected over the entire range in x. As before, the carbon signal varies between 2×10^{14} and 2×10^{15} cm^{-3}, showing no systematic dependence on the Si content. The resonance of the Ge dangling bonds exhibits the same behavior as at room temperature, rising to a pronounced peak around $x(s)=0.08$ and then falling off to a level of about 2×10^{15} cm^{-3} near the detection limit for higher Si content. This low density of Ge dangling bonds [approxi-

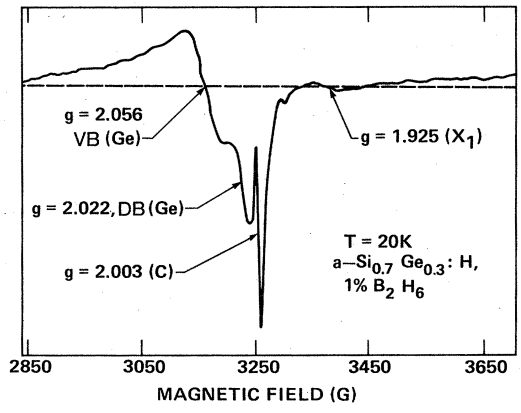

FIG. 2. Low-temperature ($T=20$ K) ESR spectrum of a-$Si_{0.7}Ge_{0.3}$:H doped with 1 vol % boron. The four resonances are due to localized holes [VB(Ge), $g=2.056$], dangling bonds [DB(Ge), $g=2.022$], carbon impurities (C, $g=2.003$), and the new X_1 states at $g=1.925$.

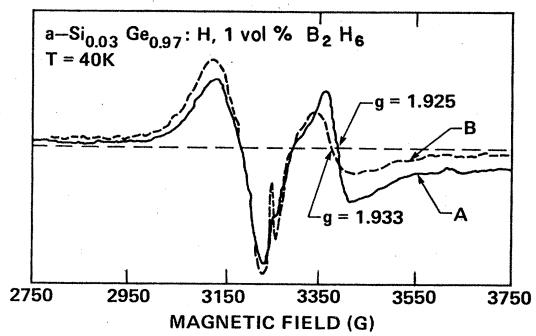

FIG. 3. ESR spectrum of boron-doped a-$Si_{0.03}Ge_{0.97}$:H. A, as-deposited; B, after exposure to diluted HCl for 10 min.

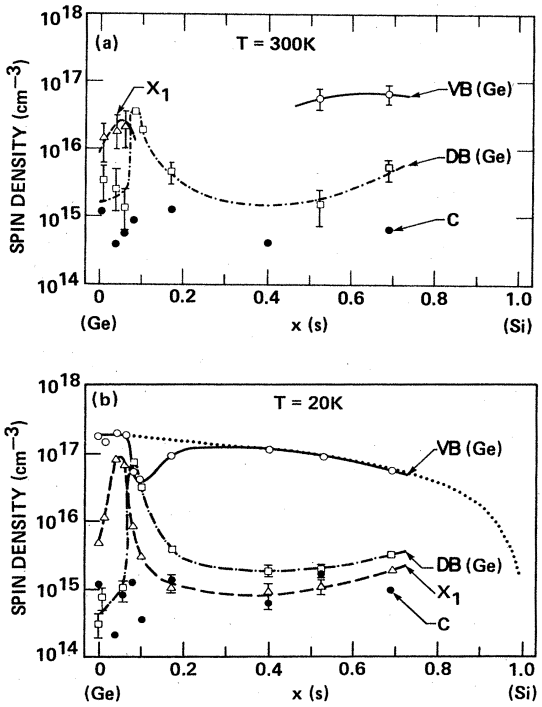

FIG. 4. Dependence of the spin density of the four different ESR signals in Fig. 2 on alloy composition $x(s)$: (a) at room temperature; (b) at $T=20$ K. The dotted line in (b) indicates the relative decrease in germanium content $[1-x(s)]$.

mately 2 orders of magnitude lower than in pure undoped a-Ge:H (Ref. 26)] is mostly due to the boron doping: The Fermi level is shifted into the valence-band tail, leaving the dangling-bond states unoccupied. A behavior similar to that of the Ge dangling bonds is observed for the X_1 signal, only here the peak in spin density (10^{17} cm^{-3}) is located at even smaller Si contents, $x(s)=0.04$. Both the X_1 and the Ge dangling-bond resonance seem to rise again as $x(s)$ reaches the silicon-rich side of composition. The strong increase of the density of dangling bonds at $x(s)=0.08$ leads to a pronounced shift of the Fermi level towards midgap. This can be seen by the changes in the spin density of the Ge valence-band tail signal. For small $x(s)$ the same spin density as in pure a-Ge:H ($N_s=2\times10^{17}$ cm^{-3}) is obtained. As the Fermi level is shifted away from the band tail around $x=0.08$, the spin density drops by nearly an order of magnitude. For higher Si content the signal intensity recovers parallel to the decay of the dangling-bond resonance. For $x(s)>0.3$ the spin density finally follows the Ge content $1-x(s)$, as indicated by the dotted line in Fig. 4(b).

Even at the lower temperature no sign of any signal connected to silicon states can be observed. Owing to the similar linewidths and g values, the presence of a Si dangling-bond signal could be masked by the carbon impurities. Therefore only an upper limit of $N_s<2\times10^{15}$ cm^{-3} can be deduced for Si dangling bonds. Nevertheless, even this upper limit seems small when compared to pure boron-doped a-Si:H prepared in the same system. Those samples show Si dangling bonds with a density of at least 4×10^5 cm^{-3}.[25] Finally, by comparing Figs. 4(a) and 4(b) it can be noticed that the different resonances show no significant temperature dependence as far as their spin densities between 20 and 300 K is concerned.

IV. DISCUSSION

A. Defect density and alloy composition

A discussion of the defect density must include the composition dependence of the dangling-bond and the X_1 resonance, since they are closely related to the amount of bulk and surface defects present in the film. From Fig. 4 it becomes immediately evident that both bulk- and surface-defect densities are increased significantly around $x=0.08$. To investigate this connection between alloy composition and defect density further, it is useful to examine the silicon content $x(s)$ in the deposited film as a function of the silicon content $x(g)$ in the plasma of the glow discharge. The quantities $x(s)$ and $x(g)$ are connected by the relation

$$1-1/x(s)=[p(\mathrm{Ge})/p(\mathrm{Si})][1-1/x(g)]\ , \qquad (2)$$

where $p(Y)$ is the overall probability of a Ge or Si atom for being incorporated into the solid film. In Fig. 5 the Si content $x(s)$ in the solid is again shown as a function of $x(g)$. For small values of $x(g)$ (<0.05) the experimental curve follows, within the estimated error, the theoretical curve for equal incorporation probabilities, $p(\mathrm{Ge})=p(\mathrm{Si})$, and therefore $x(s)=x(g)$. For $x(g)>0.1$, however, the incorporation of a Ge atom into the alloy becomes much more favorable, as can be seen in Fig. 5, where $x(s)$ as a function of $x(g)$ follows quite accurately the empirical curve $p(\mathrm{Ge})=5p(\mathrm{Si})$. This result is confirmed strongly by the fact that under similar deposition conditions, the deposition rates of pure amorphous Ge and Si films differ by a factor of approximately 5.[13,30] This behavior is commonly explained as resulting from the difference between the H_3Ge—H and H_3Si—H bonding energies (87 kcal/mol in germane[32] and 94 kcal/mol in silane[33]). The difference of about 7 kcal/mol could well account for a 5-times-higher deposition rate for germanium due to a higher concentration of the rate-limiting radicals in the plasma. In this simple model, however, one would expect the same preferential incorporation of Ge independent of the gas-phase ratio $x(g)/[1-x(g)]$. This is not observed experimentally. Instead, Fig. 6(a) shows that the ratio $p(\mathrm{Ge})/p(\mathrm{Si})$ of the incorporation probabilities drops around $x(g)=0.06$ from the value 5 to an equal incorporation probability for Ge and Si atoms. Moreover, Fig. 6(b) demonstrates that for the same value of $x(g)$ both defect-related ESR resonances (Ge dangling bond and X_1) reach their maximum spin density and fall off for higher SiH_4 content parallel to the increase of $p(\mathrm{Ge})/p(\mathrm{Si})$. On the silicon-rich side of plasma composition there is no indication of a similar phenomenon.

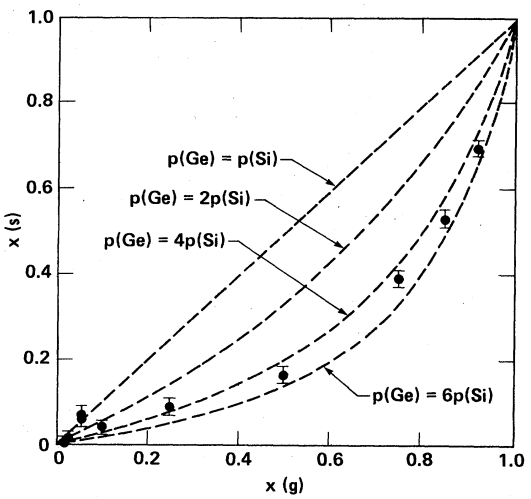

FIG. 5. Theoretical variation of the silicon content $x(s)$ in the solid with that in the plasma, $x(g)$, for different ratios $p(\mathrm{Ge})/p(\mathrm{Si})$ of the incorporation probabilities according to Eq. (2). The points are the experimental results as obtained by EPMA.

For an explanation of these results two different approaches seem possible. The total incorporation probability $p(Y)$ as defined in Eq. (2) can be written as

$$p(Y)=\sum_n p_g(Y_n)p_s(Y_n),\quad Y=\mathrm{Si,Ge}\ . \qquad (3)$$

Here, $p_g(Y_n)$ is the probability of a Si or Ge atom in the stable plasma to belong to the species Y_n (e.g., SiH_3, GeH_2, or Si_2H_5), and $p_s(Y_n)$ is the probability for such an atom to be bound into the growing solid film via the deposition of this species. By definition, the probabilities

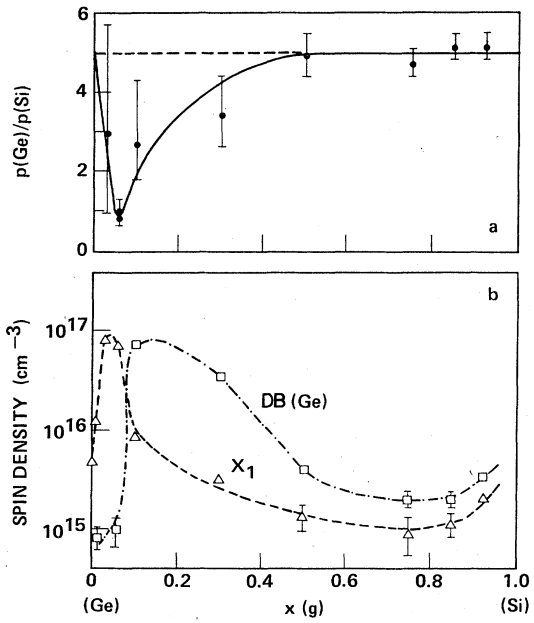

FIG. 6. (a) Ratio p(Ge)/p(Si) of the incorporation probabilities for germanium and silicon, and (b) spin density of the Ge dangling-bond and X_1 resonances as a function of the silane content $x(g)$.

p_g are a function of $x(g)$, whereas the p_s are a function of $x(s)$ only. Within this model the experimental data in Fig. 6 indicate the existence of at least one critical composition either for the gas phase $[x(g)]$ or the solid phase $[x(s)]$. A critical gas-phase composition would manifest itself by an increase of one or more of the probabilities $p_g(\mathrm{Si}_n)$ relative to the factors $p_g(\mathrm{Ge}_n)$, thus leading to the observed decrease of p(Ge)/p(Si). The corresponding increase in defect density could in this case be linked to a subsequent change in the growth mechanism.

On the other hand, the same decrease of p(Ge)/p(Si) can be explained by an increase of the probabilities $p_s(\mathrm{Si}_n)$ only, i.e., by a critical composition $x(s)$ of the solid. This could lead again to an increase of the defect density as observed experimentally. The existence of a critical alloy composition is reminiscent of a similar behavior commonly found in crystalline Si-Ge alloys. Here, critical compositions are observed around $x=0.15$ and 0.9. These values separate the range where single crystals can be grown easily from the range where only polycrystalline samples are obtained.[34,35]

The most promising approach to discern between these two possibilities seems to be an investigation of the glow-discharge plasma for different [SiH_4]:[GeH_4] ratios. This, however, is beyond the scope of this paper. Another question that remains to be answered is whether a similar critical composition exists for large $x(s)$ or $x(g)$. Here, a close investigation of the region $0.93<x(s)<1$ $[0.75<x(g)<1]$ would be necessary. The only study known to us covering this compositional range sufficiently is that of Hauschildt *et al.*[3] for undoped *a*-Si_xGe_{1-x}:H. They find pronounced changes in the optical and electrical properties of their samples for $0<x(s)<0.1$, and a less critical dependence on $x(s)$ for the silicon-rich alloys $[0.85<x(s)<1]$, again indicating the existence of one critical composition on the germanium-rich side.

B. Electronic density of states

We will now discuss the implications of the present study on the understanding of the electronic density of states in Si_xGe_{1-x}:H alloys. The discussion will be based on the current models for the DOS in the pure materials, i.e., *a*-Ge:H and *a*-Si:H, as inferred from ESR, photoemission, deep-level transient spectroscopy, and other measurements. While the qualitative features of the DOS are more or less agreed upon, the quantitative values remain a subject of continued controversy. Before discussing the DOS of the alloy system we will therefore specify the DOS model used for the pure materials. However, only the qualitative differences between *a*-Si:H and *a*-Ge:H will be important for the following discussion.

The points of reference for the amorphous materials are the mobility edges E_c and E_v of the conduction and valence bands. The mobility gap E_c-E_v amounts to about 1.0 eV for *a*-Ge:H and 1.7 eV for *a*-Si:H. In both materials the tailing of the bands into the mobility gap is very similar. Characteristic values for the extension of the tails into the gap are 0.4 eV for the valence band and 0.25 eV for the conduction band. In both materials the dominating defect states are the dangling bonds. The energetic separation of the singly occupied dangling-bond state (D^0) from E_v is again similar (0.5—0.6 eV) in *a*-Si:H and *a*-Ge:H.[26,36] A major difference is introduced by the different correlation energies U in *a*-Ge:H ($U=0.1$ eV) and *a*-Si:H ($U=0.3$ eV), which lead to a position of the doubly occupied D^- defect state at 0.65 and 0.9 eV above E_v, respectively.

In order to obtain a common scale for the energies, an absolute value for a significant energy level must be established. A suitable quantity is the energy of the valence-band maximum with respect to the vacuum level, i.e., the ionization energy, which can be measured by photoemission. For crystalline Si and Ge a series of experimental and theoretical studies exists (Refs. 37 and 38, and references therein), which place the valence-band maximum (VBM) consistently at (-4.80 ± 0.1) eV for germanium and at (-5.10 ± 0.1) eV for silicon (zero of energy equals vacuum level). A somewhat lower value is found for the mobility edge of the valence band in *a*-Si:H deposited at 220 °C: $E_v(\mathrm{Si})=(-5.6\pm0.2)$ eV.[36] No similar high-resolution XPS study for *a*-Ge:H exists so far, but it is reasonable to assume that the corresponding value for E_v(Ge) is shifted from the crystalline VBM toward lower energies in a similar way. Tentatively, a value of $E_v(\mathrm{Ge})=-5.1$ eV is proposed here to explain the ESR data.

The simplest model for the DOS in the Ge-Si alloy is obtained from the DOS of pure *a*-Ge:H and *a*-Si:H by taking a weighted average according to the composition $x(s)$. This leads to the DOS shown in Fig. 7. This simple model can explain the linear variation of the optical gap,[1,3,7,16,39] the positions of the Fermi level,[5] and the

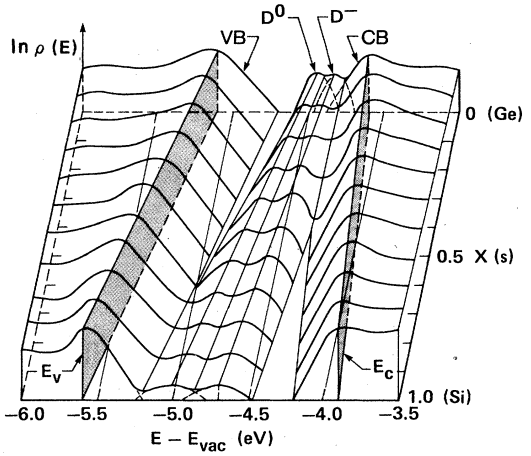

FIG. 7. Model for the density of states in a-Si_xGe_{1-x} obtained by averaging between the pure a-Ge:H and a-Si:H DOS. (E_{vac}, vacuum level; E_c, E_v, mobility edges; VB,CB, tail of the valence and conduction bands; D^0,D^-, singly and doubly occupied dangling-bond defect states.)

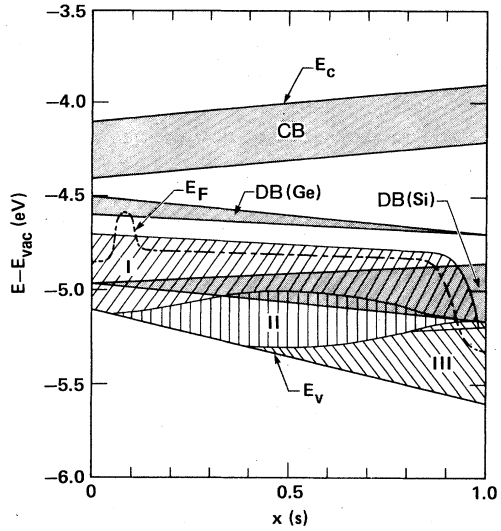

FIG. 8. Proposed model for the density of states in a-Si_xGe_{1-x}:H prepared by glow discharge as a function of alloy composition. [CB, localized conduction-band-tail states; DB(Ge),DB(Si), singly occupied dangling bonds at Ge and Si atoms; I-III, localized valence-band-tail states due to Ge—Ge bonds (I), Ge—Si bonds (II), and Si—Si bonds (III).] The dashed-dotted line shows the approximate position of the Fermi level in samples with 1 vol % boron doping.

behavior of the ESR parameters (g value and linewidth) in high-defect-density samples[17,21] with $x(s)$. A DOS such as the one in Fig. 7 is to be expected in first order for electronic states that have a sufficient overlap with neighboring states. Then the average potential of a larger region rather than the specific local potential around a given atom will determine the electronic properties. We expect such an approximation to be valid for the weakly localized antibonding states forming the conduction-band tail and for the dangling-bond defect states in the case of a very high defect density ($N_s > 10^{19}$ cm^{-3}), where the electronic wave functions have a sufficient overlap.

A different behavior should be observed, however, for the low dangling-bond density in a-Si_xGe_{1-x}:H prepared by glow discharge and for the much more localized states of the valence-band tail. Indeed, ESR spectra of undoped a-Si_xGe_{1-x}:H with low dangling-bond concentrations no longer show an average signal, but rather a structured resonance resembling an additive superposition of the characteristic Si and Ge dangling-bond spectra.[20,22] In this case the model of Fig. 7 will no longer be a valid approximation and should be replaced by a model that can explain the coexistence of germanium-like and silicon-like states at any composition of the alloy.

Such a model is outlined schematically in Fig. 8. For the conduction-band tail (CB) a similar average behavior as in Fig. 7 has been assumed because of the small degree of localization of the wave functions. The other extreme, i.e., an energetic position nearly independent of alloy composition, is used to describe the approximate dangling-bond DOS, since the corresponding wave functions are strongly localized[27] and therefore less sensitive to changes of the nearest-neighbor atoms. The dangling-bond density will thus depend only on the number of Ge or Si atoms present in the sample without shifting much in energy. This is indicated in Fig. 8 by the narrowing of the bands representing these defect states.

A more complicated structure is to be expected for the electronic states of the valence-band tail. These states are bonding states of weak bonds and, although they are fairly localized, will depend on the kind of nearest-neighbor atoms a given atom is bonding to. In the extreme case of strong localization one might then divide the valence-band tail into three regions: Ge—Ge bonding states (I), Ge—Si bonding states (II), and Si—Si bonding states (III), the number of which varies with alloy composition according to Eqs. (1a)—(1c).

Although this model for the DOS in a-Si_xGe_{1-x}:H is still rather crude, it can account qualitatively for many experimental observations in a consistent way. We begin by noticing that the model still predicts an approximately linear increase for the energy of optical transitions (absorption, photoluminescence) with $x(s)$. The main differences between Fig. 8 and the simple model in Fig. 7 are the following:

(i) The separation of the Ge and Si dangling-bond energy levels. This is necessary to explain the ESR response observed in undoped samples with low defect densities (see above).

(ii) The introduction of a band of deep hole traps in the energy range $0.3 < E - E_v < 0.7$ eV for silicon-rich samples due to the existence of a considerable amount of Ge—Ge bonding states up to $x(s) = 0.9$. These additional states should lead to an extra absorption band in the energy range $0.7 < h\nu < 1.3$ eV for $x(s) > 0.3$ and to a broadening of the photoluminescence peak in alloys with large silicon content. Indeed, both phenomena are observed experimentally.[3,7] Moreover, the model in Fig. 8 allows a qualitative explanation of the ESR results report-

ed here for boron-doped samples. For small silicon content the Fermi level lies inside the germanium valence-band tail, and mainly localized holes in Ge—Ge bonding states are observed in the ESR spectra. Around $x=0.08$ the sudden increase in defects (cf. Fig. 6) shifts E_F into a position between the Ge dangling bonds and the valence-band tail. It is estimated from the combined intensity of the two corresponding ESR signals that as many as 10^{19} to 10^{20} Ge dangling bonds per cubic centimeter are present in the samples at this composition. With the decay of this large defect density for higher silicon content, the Fermi level returns to the Ge valence-band tail and remains fixed there in a position relatively independent of $x(s)$ by the Ge—Ge bonding states which are still abundantly present in the material up to very high silicon content. (A germanium content of only 10 at.% translates into a density of Ge—Ge bonding states of the order of 10^{21} cm^{-3}). This position of the Fermi level explains why neither silicon dangling bonds nor silicon valence-band-tail states can be observed in the ESR spectra. In addition, the temperature dependence of the ESR signal due to the holes in Ge—Ge bonding states should be significantly reduced. This dependence is closely related to the interaction between the localized holes and holes in extended states below E_v.[40] Since according to Fig. 8 the distance between E_F and E_v increases with increasing $x(s)$ up to $x(s)=0.8$, the number of holes in the extended states will be significantly reduced. Therefore it is expected that the Ge valence-band-tail resonance will become less and less temperature dependent as $x(s)$ increases. This is again verified experimentally (see Fig. 4): For $x(s)>0.5$ the ESR signals of the localized holes are nearly identical at 20 and 300 K, whereas below $x(s)=0.5$ no signal at all can be observed at room temperature.

Finally, for the highest silicon content a rapid drop of the Fermi level into the band of Si—Si bonding states is predicted. In this alloy region the silicon dangling bonds and subsequently the localized holes in the Si—Si bonds should be observed by ESR. Unfortunately, the corresponding samples [$x(g)>0.95$] were not available for the present study, so that an investigation of this interesting alloy range remains a subject for future experiment.

V. CONCLUSIONS

The present study has shown the possibility of preparing boron-doped a-Si_xGe_{1-x}:H by glow discharge over the range $0<x<0.7$ without detectable phase separation or microcrystallinity. It is found that the incorporation probability of Ge as compared to that of Si is enhanced by a factor of approximately 5. However, a critical alloy composition exists at low silicon content, characterized by an equal incorporation probability for the two constituents and a strong increase in the defect density as observed by ESR. The ESR measurements lead to the proposition of a model for the density of states in a-Si_xGe_{1-x}:H containing two important features: First, because of the low defect density in the material, the Si and Ge dangling-bond states are expected to belong to two distinct bands as opposed to an average defect band observed in highly defective material. Second, it is suggested that the Ge—Ge bonding states form an additional band of hole traps in samples with a silicon content larger than 30 at.%. This band pins the Fermi level in Ge-like states for $x<0.8$, thus preventing the observation of an ESR resonance related to Si-like states in the compositional range investigated.

ACKNOWLEDGMENTS

We would like to thank H. Dersch for the preparation of most of the samples, J. B. Boyce for NMR measurements, and L. Fennell for performing the microanalysis. Stimulating discussions with D. K. Biegelsen and R. A. Street are gratefully acknowledged. This study was made possible by the Deutsche Forschungsgemeinschaft and Stiftung Volkswagenwerk, and was partly supported by the Solar Energy Research Institute (Golden, Colorado) under Contract No. XB-3-03112-1.

[1]J. Chevallier, H. Wieder, A. Anton, and C. R. Guarnieri, Solid State Commun. **24**, 867 (1977).
[2]P. O'Connor and J. Tauc, Phys. Rev. Lett. **43**, 311 (1979).
[3]D. Hauschildt, R. Fischer, and W. Fuhs, Phys. Status Solidi (B) **102**, 563 (1980).
[4]G. Nakamura, K. Sato, Y. Yukimoto, K. Shirahata, T. Murahashi, and K. Fujiwara, Jpn. J. Appl. Phys. Suppl. **20-1**, 291 (1981).
[5]Nguyen Van Dong, Tran Huu Danh, and J. Y. Leny, J. Appl. Phys. **52**, 338 (1981).
[6]P. O'Connor and J. Tauc, Phys. Rev. B **25**, 2748 (1982).
[7]B. von Roedern, D. K. Paul, J. Blake, R. W. Collins, G. Moddel, and W. Paul, Phys. Rev. B **25**, 7678 (1982).
[8]P. K. Banerjee, R. Dutta, S. S. Mitra, and D. K. Paul, J. Non-Cryst. Solids **50**, 1 (1982).
[9]G. Nakamura, K. Sato, and Y. Yukimoto, Sol. Cells **9**, 75 (1983).
[10]N. J. Shevchick, J. S. Lannin, and J. Tejeda, Phys. Rev. B **7**, 3987 (1973).
[11]K. L. Chopra, H. S. Randhawa, and L. K. Malhotra, Thin Solid Films **47**, 203 (1977).
[12]S. Hasegawa, S. Yazaki, and T. Shimizu, J. Non-Cryst. Solids **27**, 215 (1978).
[13]D. K. Paul, B. von Roedern, S. Oguz, J. Blake, and W. Paul, J. Phys. Soc. Jpn. Suppl. A **49**, 1261 (1980).
[14]W. Paul, D. K. Paul, B. von Roedern, J. Blake, and S. Oguz, Phys. Rev. Lett. **46**, 1016 (1981).
[15]J. C. C. Fan and C. H. Anderson, Jr., J. Appl. Phys. **52**, 4003 (1981).
[16]G. Lucovsky, S. S. Chao, J. E. Tyler, and G. DiMaggio, J. Vac. Sci. Technol. **21**, 838 (1982).
[17]M. Kumeda, Y. Jinno, and T. Shimizu, Phys. Status Solidi (B)

81, K71 (1977).
[18]S. Hasegawa, S. Yazaki, and T. Shimizu, Solid State Commun. **23**, 901 (1977).
[19]J. Dumas, Phys. Status Solidi (B) **86**, K75 (1978).
[20]T. Shimizu, M. Kumeda, and Y. Kiriyama, in *Tetrahedrally Bonded Amorphous Semiconductors (Carefree, Arizona),* A Topical Conference on Tetrahedrally Bonded Amorphous Semiconductors, edited by R. A. Street, D. K. Biegelsen, and J. C. Knights (AIP, New York, 1981), p. 171.
[21]T. Shimizu, M. Kumeda, and Y. Kiriyama, Solid State Commun. **37**, 699 (1981).
[22]A. Morimoto, T. Miura, M. Kumeda, and T. Shimizu, Jpn. J. Appl. Phys. **20**, L833 (1981).
[23]K. Murase, A. Takeda, and Y. Mizushima, Jpn. J. Appl. Phys. **21**, 561 (1982).
[24]R. A. Street and D. K. Biegelsen, Solid State Commun. **33**, 1159 (1980).
[25]H. Dersch, J. Stuke, and J. Beichler, Phys. Status Solidi (B) **105**, 265 (1981).
[26]M. Stutzmann, J. Stuke, and H. Dersch, Phys. Status Solidi (B) **115**, 141 (1983).
[27]M. Stutzmann and J. Stuke, Solid State Commun. **47**, 635 (1983).
[28]R. J. Nemanich and J. C. Knights, J. Non-Cryst. Solids **35-36**, 243 (1980).
[29]R. M. White, J. Non-Cryst. Solids **16**, 387 (1974).
[30]D. P. Galley, M.S. thesis, University of Delaware, 1983 (unpublished).
[31]M. Stutzmann and J. Stuke, J. Non-Cryst. Solids **66**, 145 (1984).
[32]*Handbook of Chemistry,* 12th ed., edited by J. A. Dean (McGraw-Hill, New York, 1978), pp. 3—129.
[33]*CRC Handbook of Chemistry and Physics,* 60th ed., edited by R. C. West (The Chemical Rubber Co., Cleveland, Ohio, 1980), p. F-233.
[34]E. R. Johnson and S. M. Christian, Phys. Rev. **95**, 560 (1954).
[35]R. Braunstein, A. R. Moore, and F. Herman, Phys. Rev. **109**, 695 (1958).
[36]S. Griep and L. Ley, J. Non-Cryst. Solids **59-60**, 253 (1983).
[37]G. W. Gobeli and F. G. Allen, Phys. Rev. **137**, A245 (1965).
[38]K. Unger and H. Neumann, Ann. Phys. (N.Y.) **38**, 291 (1981).
[39]K. Shimakawa, J. Non-Cryst. Solids **43**, 229 (1981).
[40]M. Stutzmann and J. Stuke, Phys. Status Solidi (B) **120**, 225 (1983).